

# Tracking Vital Signs During Sleep Leveraging Off-the-shelf WiFi

Jian Liu<sup>†</sup>, Yan Wang<sup>†</sup>, Yingying Chen<sup>†</sup>, Jie Yang<sup>\*</sup>, Xu Chen<sup>†</sup>, Jerry Cheng<sup>§</sup>

<sup>†</sup>Stevens Institute of Technology, Hoboken, NJ 07030, USA

<sup>\*</sup>Florida State University, Tallahassee, FL 32306, USA

<sup>§</sup>Rutgers University, North Brunswick, NJ 08902, USA

†{jliu28, ywang48, yingying.chen}@stevens.edu, \*jyang5@fsu.edu, †xchen30@stevens.edu, §jcheng1@rwjms.rutgers.edu

## ABSTRACT

Tracking human vital signs of breathing and heart rates during sleep is important as it can help to assess the general physical health of a person and provide useful clues for diagnosing possible diseases. Traditional approaches (e.g., Polysomnography (PSG)) are limited to clinic usage. Recent radio frequency (RF) based approaches require specialized devices or dedicated wireless sensors and are only able to track breathing rate. In this work, we propose to track the vital signs of both breathing rate and heart rate during sleep by using off-the-shelf WiFi without any wearable or dedicated devices. Our system re-uses existing WiFi network and exploits the fine-grained channel information to capture the minute movements caused by breathing and heart beats. Our system thus has the potential to be widely deployed and perform continuous long-term monitoring. The developed algorithm makes use of the channel information in both time and frequency domain to estimate breathing and heart rates, and it works well when either individual or two persons are in bed. Our extensive experiments demonstrate that our system can accurately capture vital signs during sleep under realistic settings, and achieve comparable or even better performance comparing to traditional and existing approaches, which is a strong indication of providing non-invasive, continuous fine-grained vital signs monitoring without any additional cost.

## Categories and Subject Descriptors

H.4 [Information Systems Applications]: Miscellaneous

## Keywords

Vital Signs; Channel State Information (CSI); WiFi; Sleep Monitoring

## 1. INTRODUCTION

Vital signs, such as breathing rate and heart rate, indicate the state of a person's essential body functions. They are the essential components to assess the general physical health of a person and identify various disease problems. Correlating

the vital signs with our sleep quality can further enable sleep apnea diagnosis and treatment [1], treatment for asthma [2] and sleep stage detection [3]. However, the traditional way to monitor vital signs during sleep requires a patient to perform hospital visits and wear dedicated sensors [4], which are intrusive and costly. The obtained results may be biased because of the unfamiliar sleeping environments in the hospital. Moreover, it is difficult, if not possible, to run long-term sleep monitoring in clinical settings. Thus, a solution that can provide non-invasive, low-cost and long-term vital signs monitoring without requiring hospital visits is highly desirable.

Recently, Radio Frequency (RF) based monitoring solutions [5, 6, 7, 8] have drawn considerable attention as they provide non-invasive breathing rate monitoring. For example, F. Adib et al. utilize Universal Software Radio Peripheral (USRP) and Frequency Modulated Continuous Wave (FMCW) radar to monitor a person's breathing rate by detecting the chest fluctuations caused by breathing [7, 8]. Doppler radar [5] and ultra-band radar [6] are utilized to catch a person's breathing respectively. These systems involve specialized devices with high complexity, which prevent them from large-scale and long-term deployment. Furthermore, N. Patwari et al. [9, 10] use coarse-grained channel information (i.e., received signal strength (RSS)) extracted from wireless sensor nodes to detect breathing rate. Their approach requires additional wireless network infrastructure (i.e., dedicated sensor nodes), and the coarse-grained channel information is not able to capture the vital signs of heart rate. Another new direction is using wearable sensors (such as Fitbit [11] and Jawbone [12]) to track people's fitness at any time. But they only have the capability of performing coarse-grained sleep monitoring without capturing the breathing rate, which is critical to many sleep problem diagnosis including sleep apnea. Additionally, users are required to wear these fitness sensors even during their sleep, which could be a challenge for elder people.

To address these issues, our work aims to perform continuous long-term vital signs monitoring with low cost and without the requirement of wearing any sensor. We show that it is possible to track breathing rate and heart rate during sleep by using off-the-shelf WiFi. This will largely increase the opportunity for wide deployment and in-home use. Indeed, our system re-uses existing WiFi network for tracking vital signs without dedicated/wearable sensors or additional wireless infrastructure. Furthermore, by exploiting fine-grained channel information, Channel State Information (CSI), provided by off-the-shelf WiFi device, our system captures not

Permission to make digital or hard copies of all or part of this work for personal or classroom use is granted without fee provided that copies are not made or distributed for profit or commercial advantage and that copies bear this notice and the full citation on the first page. Copyrights for components of this work owned by others than ACM must be honored. Abstracting with credit is permitted. To copy otherwise, or republish, to post on servers or to redistribute to lists, requires prior specific permission and/or a fee. Request permissions from [permissions@acm.org](mailto:permissions@acm.org).

*MobiHoc'15*, June 22–25, 2015, Hangzhou, China.

Copyright © 2015 ACM 978-1-4503-3489-1/15/06 ...\$15.00.

<http://dx.doi.org/10.1145/2746285.2746303>.

only the breathing rate but also heart rate. Specifically, our system utilizes the readily available channel information to detect the minute movements caused by breathing and heart beats (i.e., inhaling, exhaling, diastole and systole).

Using channel state information has significant implication on how fine-grained minute movements can be captured for vital signs monitoring. Comparing to the traditional RSS, which only provides a single measurement of the power over the whole channel bandwidth, the fine-grained CSI provides both amplitude and phase information for multiple OFDM subcarriers. For instance, the mainstream WiFi systems such as 802.11 a/g/n are based on OFDM where the relatively wideband 20MHz channel is partitioned into 52 subcarriers. Due to the frequency diversity of these narrowband subcarriers, the multipath effect and shadow fading at different subcarriers may result in significant difference in the observed amplitudes. This means that a small movement in physical environment may lead to the change of CSI at some subcarriers, whereas such change maybe smoothed out if we examine the signal strength over the whole channel bandwidth. Our system thus takes advantage of the fine-grained CSI provided by off-the-shelf WiFi device to capture the minute movements for vital signs monitoring.

Our system uses only a single pair of WiFi device and wireless AP for detecting the breathing rate and heart rate during sleep. The breathing rate detection algorithm first obtains time series of CSI from off-the-shelf WiFi device (e.g., desktop, laptop, tablet, and smartphone) and then analyzes the information in time domain and frequency domain. It achieves high accuracy for both single and two-person in bed scenarios. To detect heart rate, our algorithm first applies a bandpass filter to eliminate irrelevant frequency components, and then estimates the heart rate in the frequency domain by locating the frequency peak in the normal heart rate range. Extensive experiments are conducted in lab environment and two apartments with difference sizes. The results show that our system provides accurate breathing rate and heart rate estimation not only under typical settings but also covering challenging scenarios including long distance between the WiFi device and AP, none-line-of-sight (NLOS) situation and different sleep postures. This demonstrates that our approach can provide device-free, continuous fine-grained vital signs monitoring without any additional cost. It has the capability to support large-scale deployment and long-term vital signs monitoring in non-clinical settings.

The main contributions of our work are summarized as follows:

- We show that the existing WiFi network can be re-used to capture vital signs of breathing rate and heart rate through using only one AP and a single WiFi device. Such an approach can also be extended to non-sleep scenarios when the user is stationary.
- Our proposed system extracts fine-grained channel state information (CSI) from off-the-shelf WiFi device to detect the minute movements and provide accurate breathing and heart rates estimation concurrently.
- We develop algorithms that have the capability to track breathing rates of a single person as well as two-person in bed cases, which cover typical in-home scenarios.
- Extensive experiments in both lab and two apartments over a three-month period show that our system can achieve comparable or even better performance as compared to existing dedicated sensor based approaches.

## 2. RELATED WORK

Breathing rate, heart rate and statistics of sleep events are important indicators for evaluating one's sleep quality, stress level and various health conditions. In general, the methods used to track such information during sleep can be categorized into four groups: dedicated sensor based, smartphone and wearable sensor based, touch-free sensor based and RF signal based.

Traditional approaches use dedicated sensors to measure vital signs during sleep. For example, Polysomnography (PSG) [4] measures body functions including breathing rate, eye movements (EOG), heart rhythm (ECG) and muscle activity by attaching multiple sensors to a patient. Such systems incur high cost and are usually limited to clinical usage. Recent advances of smartphones and wearable sensors have enabled in-home sleep monitoring by utilizing the built-in accelerometer and microphone [13, 14, 11, 12]. These methods mainly provide coarse-grained monitoring including the detection of body movements, snoring, or regular sleep events, and are not able to monitor breathing rate, which is a critical indication of sleep irregularity such as sleep apnea. They also require users to place smartphones close-by and wear sensors during sleep. Touch-free sensor based solutions either use the sensors attached to the mattress [15] or install a camera to capture the chest movement for breathing rate estimation [16]. These systems however require professional installations and cannot estimate heart rate.

Most related to our work is the RF signal based monitoring mechanisms, such as the use of Doppler radar [5], ultra-wideband [6], Frequency Modulated Continuous Wave (FMCW) radar [8, 7] or Received Signal Strength (RSS) [9, 10] for monitoring the vital signs of breathing rate. In particular, these mechanisms [5, 6, 7, 8] rely on specialized hardware including Universal Software Radio Peripheral (USRP), FMCW radar and Doppler radar. These systems incur high cost and high complexity, making them impractical for large scale deployment. N. Patwari et al. [9, 10] use received signal strength (RSS) measurements (e.g., using 16 frequency channels in IEEE 802.15.4) extracted from wireless sensor nodes to detect the breathing rate. Their approaches require additional wireless network infrastructure and high-density placement of sensor nodes. And the coarse-grained channel information of RSS is not able to capture the heart rate.

Different from the previous work, our system re-uses existing WiFi network for tracking vital signs of breathing and heart rates concurrently without dedicated/wearable sensors or additional wireless infrastructure. By exploiting fine-grained channel state information provided by off-the-shelf WiFi devices, our system captures both the breathing rate as well as heart rate. Our system thus performs device-free, continuous fine-grained vital signs monitoring without any additional cost. It has the potential to be widely deployed in home and many other non-clinical environments.

## 3. SYSTEM DESIGN

In this section, we discuss the preliminaries, design challenges and overview of our system design.

### 3.1 Preliminaries

While proliferating WiFi networks are usually used for wireless Internet access and connecting local area networks, such as an in-home WiFi network involving both mobile and stationary devices (e.g., laptop, smartphone, tablet, desktop, smartTV), they have great potential to sense the environment changes and capture the minute movements caused by

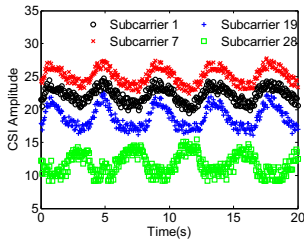


**Figure 1: CSI amplitude of four subcarriers over time when a person is asleep.**

human body [17]. Indeed, WiFi signals are affected by human body movements at various scales during sleep, such as large scale movements involving going to bed and turn over, minute movements including inhaling/exhaling for breathing and diastole/systole for heart beats. By extracting and analyzing the unique characteristics of WiFi signals, we could capture and derive the semantic meanings of such movements including both breathing rate and heart beats during sleep. We are thus motivated to re-use existing WiFi network to monitor the fine-grained vital signs during sleep as it doesn't require any dedicated/wearable sensors or additional infrastructure setup.

To monitor the minute movements of breathing and heart beats, we exploit the Channel State Information (CSI) provided by off-the-shelf WiFi devices as opposed to the commonly used Received Signal Strength (RSS). While the coarse-grained channel information of RSS provides the averaged power in a received radio signal over the whole channel bandwidth, the fine-grained CSI of WiFi signal (based on OFDM) describes at each subcarrier how a signal propagates from the transmitter to the receiver and represents the combined effect of, for example, scattering, fading, and power decay with distance. For example, in 802.11 a/g/n, a relatively wideband  $20MHz$  OFDM channel (or carrier) is partitioned into 52 subcarriers. And we could examine the amplitude and phase at each subcarrier, which could be thought of as a narrowband channel, for extracting the minute movements. Due to the relative narrowband channel, the scattering and reflecting effects caused by minute movements could result in totally different amplitudes and phases at each subcarrier. Such difference however is usually smoothed out if we look at the averaged power over the whole channel bandwidth (i.e., RSS). Analyzing the CSI at each subcarrier thus provides great opportunity to capture the minute movements from not only breathing but also heart beats.

Figure 1 shows the CSI amplitude of four subcarriers (i.e., subcarrier 1, 7, 19 and 28) extracted from a laptop in a 802.11n network over time when a person is asleep. His bed is in between an AP and the laptop with 3 meters apart. The person does not carry any sensor in his body. We observe that the CSI amplitude of these four subcarriers exhibits an obvious periodic up-and-down trend. Such a pattern could be caused by the person's breathing during sleep. This observation strongly suggest that we may achieve device-free fine-grained vital signs monitoring by leveraging the CSI from off-the-shelf WiFi devices.

### 3.2 Challenges

Our goal is to track human vital signs of breathing and heart rates simultaneously using CSI measurements from a single pair of WiFi devices. To build such system under realistic settings as a typical in-home scenario, a number of challenges need to be addressed.

**Robustness to Real Environments.** The placement of WiFi devices in real environments could change over time, and different persons present different sleeping postures. Our system should be able to provide accurate vital sign monitoring under such challenging conditions including various distances between the AP and WiFi devices, presence of walls between WiFi devices (creating none-line-of-sight (NLOS) scenarios), and different sleeping postures. In addition, our system should be able to identify regular sleep related events (such as turnover or getting out of bed) to facilitate vital signs monitoring.

**Tracking Breathing & Heartbeat Simultaneously.** Both breathing and heart beat only involve small body movements, presenting significant challenges when tracking such vital signs simultaneously under realistic settings. Even if the repeatable CSI changing pattern caused by breathing could be detected as shown in Figure 1, it is difficult to capture heartbeat movements using WiFi links at the same time. Because the noisy environments will also affect CSI measurements, making it much harder to distinguish the minute movements caused by breathing (i.e., inhaling and exhaling) and heart beats (i.e., diastole and systole).

**Sensing with Single Pair of AP and WiFi Device.** Our approach should work with existing WiFi infrastructure, which may have only a single wireless link (between the AP and the device) across the human body. This presents additional challenges when two people are in-bed together. Our system should be able to distinguish and measure breathing rates coming from two people. Furthermore, the system should use WiFi traffic as little as possible, such as only utilizing existing beaconing traffic.

### 3.3 System Overview

The basic idea of our system is to track vital signs during sleep through capturing the unique patterns embedded in WiFi signals. As illustrated in Figure 2, the system takes as input time-series CSI amplitude measurements, which can be collected at an off-the-shelf WiFi device by utilizing existing WiFi traffic or system-generated periodic traffic (if network traffic is insufficient) during people's sleep. The data is then processed to filter out the CSI measurements that contain sleep events (e.g, going to bed and turn over) or large environmental changes such as people walking by via *Coarse Sleep Event Detection and Filtering*. The measurements belonging to the regular sleep events can be further classified to detailed events such as going to bed, getting off bed and turnovers. Moreover, our work is based on the fact that breathing and heart rates of resting people have different frequency ranges (e.g., breathing rate ranges from 10 to 37 bpm [18, 19], and heart rate ranges from 60 to 80 bpm [20]). This useful information leads us to work on different frequency bands of the CSI measurements for accurate vital signs estimation.

The core components of our system are *Breathing Rate Estimation* and *Heart Rate Estimation*. After coarse sleep event detection and data filtering, based on the different frequency information embedded inside the CSI measurements, the input is fed into *Breathing Rate Estimation* and *Heart Rate Estimation* respectively. In particular, the lower-frequency information of the CSI measurements is processed by the *Breathing Rate Estimation* component. Our system first performs *Data Calibration* and *Subcarrier Selection* to preprocess the data and select only the subcarriers sensitive to minute human body movements (i.e., subcarriers with



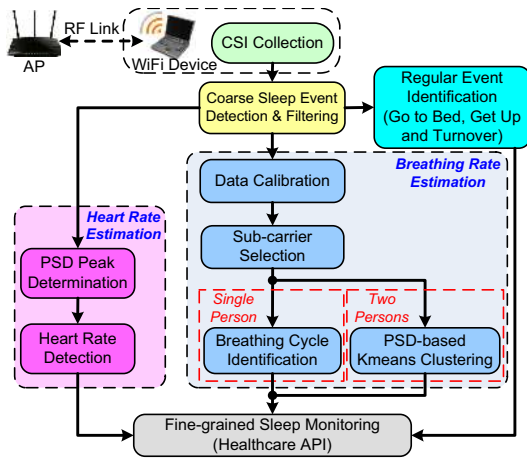


Figure 2: Overview of system flow.

large variances). We then develop two methods, *Breathing Cycle* and *PSD-based K-means Clustering*, to estimate the breathing rate for single and two-person in-bed scenarios respectively. *PSD* denotes power spectral density. Following the similar principle, *PSD-based K-means Clustering* can be easily extended to handle the case of estimating breathing rates for multiple people simultaneously given the number of people under study is known. The higher-frequency information of the CSI measurements is fed into the *Heart Rate Estimation* component. The heart rate is then derived in the frequency domain by examining the peaks in power spectral density (PSD) of CSI measurements. We leave the detailed presentation of *Breathing Rate Estimation* and *Heart Rate Estimation* to Section 4 and Section 5, respectively.

## 4. BREATHING RATE ESTIMATION

We first describe *Data Calibration* and *Subcarrier Selection*, and then present *Breathing Cycle Identification* for estimating an individual’s breathing rate. We finally show how to estimate breathing rates for two persons in-bed case.

### 4.1 Data Calibration

Data calibration is used to improve the reliability of the CSI by mitigating the noise presented in the collected CSI samples in real environments. The noise sources could come from environment-related changes, radio signal interference, etc. Our data calibration first utilizes the Hampel filter [21] to filter out the outliers which have significant different values from other neighboring CSI measurements. Specifically, we apply the Hampel filter with a sliding window at each subcarrier to remove such outliers. After that, we further apply a moving average filter, which further removes high-frequency noise that is unlikely to be caused by breathing or heart beats as the corresponding minute movements usually present in a fixed frequency range. Figure 3 illustrates the effectiveness of our data calibration by comparing the CSI amplitude before and after data calibration under a none-line-of-sight case with severe signal outliers: the CSI amplitude shown in the figure is from a single subcarrier collected from a WiFi device, which transmits/receives packets from an AP with a wall between them. As we can see from the figure, after data calibration, the sinusoidal waves in CSI amplitude can clearly reflect the periodic up-and-down chest and belly movements caused by breathing.

### 4.2 Subcarrier Selection Strategy

We observe that the amplitudes of different subcarriers have different sensitivity to inhaling and exhaling caused by

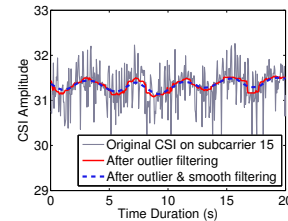
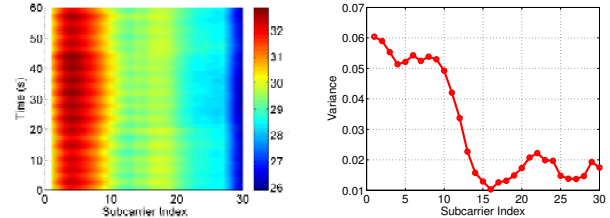


Figure 3: Illustration of data calibration of a single subcarrier.



(a) CSI time series patterns (b) Variance of each subcarrier after data calibration.

Figure 4: Example of CSI amplitude pattern at 30 subcarriers and the corresponding variance.

breathing due to frequency diversity. Figure 4(a) presents an example of CSI amplitude over time on 30 subcarriers extracted from a laptop in WiFi network when a person is asleep. We find that the CSI from the smaller subcarrier indices is significantly affected by the minute movements caused by breathing, while CSI from the higher subcarrier indices (i.e., from 15 to 30) is less sensitive. This is because different subcarriers have different central frequencies, which have different wavelengths. Combining the effect of multipath/shadowing with different frequencies, CSI measurements at different subcarriers thus have different amplitudes. Those subcarriers not sensitive to the breathing activity should be filtered out. We utilize the variance of CSI amplitude in a moving time window to quantify the subcarrier’s sensitivity to minute movements. Figure 4(b) shows the variance of 30 subcarriers. We can see that subcarriers with higher variance are more sensitive to minute movements. We thus use a threshold based method to select subcarriers having large variance of CSI amplitude in a time window for breathing rate estimation.

### 4.3 Breathing Cycle Identification

As breathing involves periodic minute movements of inhaling and exhaling, our breathing cycle identification aims to capture the periodic changes in CSI measurements caused by breathing. From Figure 1, we observe the CSI amplitude on the selected subcarrier indeed presents a sinusoidal-like periodic changing pattern over the time due to breathing. This observation suggests that we can identify breathing cycles by measuring the peak-to-peak time interval of sinusoidal CSI amplitudes. We thus first identify peaks of sinusoidal CSI amplitude patterns to calculate peak-to-peak intervals. We then combine the peak-to-peak intervals from multiple subcarriers to improve the robustness and the accuracy of breathing cycle identification.

**Local Peak Identification.** A typical peak finding algorithm determines a data sample as a peak if its value is larger than its two neighboring samples. However, such simple method produces many *fake peaks* (i.e., the identified peaks that are not at the location of real peaks of the sinusoidal CSI amplitude pattern) as illustrated in Figure 5. The

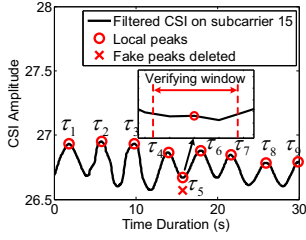


Figure 5: Illustration of fake peak removal.

peak  $\tau_5$  has larger value than its two neighboring samples, yet, it is a fake peak among these nine identified peaks. In order to filter out the fake peaks, we apply a threshold to the minimum distance between two neighboring peaks based on human’s maximum possible breathing rate. In addition, we develop a *Fake Peak Removal* algorithm to further reduce the number of fake peaks.

Specifically, adults usually breathe at 10-14 breathes per minute (bpm) [19], while new born babies breathe at around 37 bpm [18]. We therefore set the range of breathing rates being considered in our work to 10-37 bpm which covers a broad range including fast and slow breathing rates. We further adopt a minimum acceptable interval  $\sigma_{mpd}$  that corresponds to the maximum possible breathing rate as a threshold to remove the peaks that are too close to each other. If a peak has its backward interval (i.e., the interval between previous peak and current peak) less than the minimum acceptable interval length, it will be identified as a fake peak. In particular, we set the minimum acceptable interval  $\sigma_{mpd} = 60 \cdot f/37$  samples, which corresponds to the maximum possible breathing rate for infants. The parameter  $f$  is the sampling rate of CSI measurements that corresponds to WiFi packet transmission rate.

In addition, we confirm the identified peaks by comparing its value to multiple data samples within a verification window centered at the peak. The system only keeps the identified peak when its value is greater than all the data samples in the verification window. The algorithm of fake peak removal is provided in Algorithm 1. In our experiments, we observe that a short verification window of one second is good enough to remove fake peaks.

**Breathing Cycles Combination.** Once we capture all the local peaks from the selected subcarriers, a more clear pattern can be obtained as shown in Figure 6. The referenced signal is derived from the NEULOG Respiration Monitor Logger Sensor [22], which is connected to a monitor belt attached to the user’s ribcage while asleep. Next, our system estimates the breathing rate by combining peak-to-peak intervals obtained crossing all selected subcarriers. We denote a set of peak-to-peak intervals obtained from  $P$  selected subcarriers as  $L = [l_1, \dots, l_i, \dots, l_P]'$ , where  $l_i = \{l_i(1), \dots, l_i(N_i - 1)\}$  is a vector of  $N_i$  peak-to-peak intervals obtained from the  $i^{th}$  subcarrier. Then the estimated breathing cycle  $E_i$  from the  $i^{th}$  subcarrier can be obtained by using the following equation:

$$\arg \min_{E_i} \sum_{n=1}^{N_i-1} |E_i - l_i(n)|^2. \quad (1)$$

Considering the subcarriers with larger variance are more sensitive to the minute movements, we utilize a weighted mean of estimated breathing cycles crossing all selected subcarriers to obtain a more accurate estimation of breathing

---

#### Algorithm 1 Fake Peak Removal.

---

**Require:**

CSI time series on subcarrier  $i$ :  $c_i = \{c_i(1), \dots, c_i(M)\}$ ;  
Local peak set:  $MaxSet = \{\tau_k, 1 \leq k \leq K\}$ ;  
Length of the verifying window:  $N$ ;

**Ensure:**

$MaxSet$  after removing fake maximums;

- 1: **for**  $k=1: K$  **do**
  - 2:    $locs := location(\tau_k)$ ;
  - 3:    $amp := amplitude(\tau_k)$ ;
  - 4:   **for**  $m := locs - \lfloor \frac{N-1}{2} \rfloor : locs + \lfloor \frac{N-1}{2} \rfloor$  **do**
  - 5:     **if**  $m < 0 \parallel m > M$  **then**
  - 6:       **continue**;
  - 7:     **end if**
  - 8:     **if**  $amp < c_i(m)$  **then**
  - 9:       delete  $\tau_k$  from  $MaxSet$ ;
  - 10:     **break**;
  - 11:    **end if**
  - 12: **end for**
  - 13: **end for**
  - 14: **return**  $MaxSet$ ;
- 

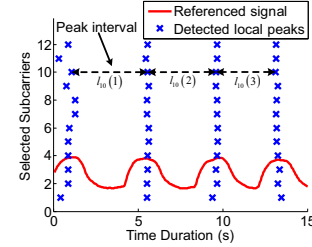


Figure 6: Local peaks of all selected subcarriers.

cycle  $E$ , which is defined as follows:

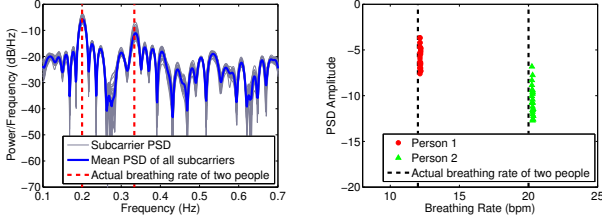
$$E = \sum_{i=1}^P \frac{\text{var}(c_i) \cdot E_i}{\sum_{i=1}^P \text{var}(c_i)}, \quad (2)$$

where  $P$  is the number of validated subcarriers,  $c_i$  is the CSI amplitude measurements on the  $i^{th}$  subcarrier. The breathing rate finally can be identified as  $60/E$  bpm.

#### 4.4 Breathing Rate Estimation of Two Persons Scenario

Estimating breathing rate becomes challenging when there are two persons in bed as the CSI measurements would be affected by two independent movements simultaneously due to breathing. It is hard to observe a clear sinusoidal pattern in the time series of CSI amplitude. Nevertheless, the frequency of the breathing coming from two persons is still preserved if we transfer the time series of CSI to the frequency domain. We therefore develop a mechanism to determine two people’s breathing rates simultaneously by examining the frequency components in CSI measurements.

In particular, our system analyzes the time series of CSI amplitude in frequency domain by using the power spectral density (PSD). The PSD transforms the time series of CSI measurements on each subcarrier to its power distribution in the frequency domain. It is used to identify the frequencies having strong signal power. A strong sinusoidal signal generates a peak at the frequency corresponding to the period of the sinusoidal signal in PSD. Therefore, the CSI amplitude measurements collected when two persons in bed should present two strong peaks at the frequency corresponding to



(a) PSD of CSI measurements. (b) K-means clustering of subcarriers' peaks.

**Figure 7: Illustration of two people breathing at different frequencies (12bpm and 20bpm).**

the breathing rate of two persons, respectively. The PSD on the  $i^{\text{th}}$  subcarrier with  $N$  CSI amplitude measurements can be calculated with following equation:

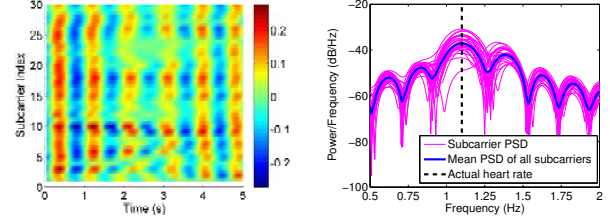
$$PSD_i = 10 \log_{10} \frac{(\text{abs}(FFT(c_i)))^2}{N}, \quad (3)$$

where  $c_i$  is the vector of CSI measurements on subcarrier  $i$ .

For each selected subcarrier, we utilize a threshold based approach to identifying the candidate peaks within its PSD. We then use a K-means clustering method to classify the candidate peaks into two clusters based on two dimensional feature including PSD amplitude and corresponding frequency. The number of targeted people (i.e.,  $K$  in K-means) can be either estimated using existing work (e.g., [23]) or entered manually from the users. The average values of the frequencies in two clusters are identified as the breathing rates of these two people. Figure 7 shows an example of estimating two persons' breathing rate using PSD based method. The ground truths of two persons' breathing rates are 12bpm and 20bpm (i.e., 0.2Hz and 0.33Hz respectively). Figure 7(a) depicts that there are two strong peaks in the PSD of selected subcarriers near these two frequencies, respectively. Figure 7(b) shows that our PSD based K-means clustering method can effectively estimate the breathing rates of two persons in bed simultaneously. We note that the proposed approach still works even when two people have the same breathing rates. Under such scenario, our approach returns two close-by PSD peaks on each selected subcarrier in the frequency domain after K-means clustering. In addition, the person's chest or belly that is closer to the wireless link has bigger impact on the CSI changes, which creates more obvious periodic changes of CSI. This leads to the stronger peak corresponds to that person's breathing or heart beat rate. We thus can map the detected breathing or heart rates to each individual based on the strength of the peak and the proximity of the individual to the wireless link.

## 5. HEART RATE ESTIMATION

Heart rate is a very important indicator of the persons' sleep status, quality and overall health condition. While the breathing patterns can be observed in the CSI measurement, the heart rates don't produce observable periodic CSI change patterns in the time series CSI measurements. This is because the vibration of blood vessels caused by heart beat (i.e., diastole and systole) are smaller minute movements than that of breathing. Thus, the effect of minute movement of heartbeat is overlapped with and covered by the chest and belly movements of breathing. On the other hand, the heartbeat has much higher frequency than breathing. We thus can filter out the interference of breathing in order to facilitate the heart rate estimation.



(a) CSI time series patterns. (b) PSD of CSI measurements on all subcarriers.

**Figure 8: Recovered heart beats by applying pass band filtering and PSD of CSI measurements.**

In particular, after Coarse Sleep Event Detection and Filtering, the CSI measurements with the frequency range related to normal heart rate range of resting people (i.e., 60bpm to 80bpm which corresponds to 1Hz to 1.33Hz) will be separated and served as input to our Heart Rate Estimation. The patterns of CSI measurements of all subcarriers after such band-pass filtering are illustrated in Figure 8(a), from which we can observe the CSI changing that accompany the heart beats. With the aid of the band-pass filter, the mean PSD curve for all subcarriers displays a noticeable peak in the PSD graph at the frequency of 1.095Hz, namely 65.7bpm, in Figure 8(b). In the same figure, there is a black dashed line representing the ground truth of 66bpm measured by a commercial fingertip pulse sensor during such time period. We then analyze the CSI amplitude on each subcarrier in frequency domain and generate the power spectral density (PSD) (refer to Equation 3) to identify the frequencies having strong signal power. We can thus determine the heart rate by locating the maximum power in the average PSD of all subcarriers in the normal heart rate range. For two person's heart rates monitoring, we can identify two heart rates simultaneously by using the similar approach to the breathing rate estimation of two persons illustrated in Section 4.4.

## 6. SYSTEM IMPLEMENTATION

### 6.1 Coarse Sleep Event Detection & Environmental Change Filtering

Coarse sleep event detection and filtering is used to detect and filter out the sleep events or environmental changes that interfere with the minute movements of breathing and heart beat during sleep. These sleep events, such as turnovers (i.e., changing sleeping postures) and getting up, and occasional changes of environments, such as people walking by, involve large scale body movements which significantly affect the CSI measurements and are irrelevant to vital signs monitoring. Our system thus performs coarse determination of CSI segments containing such inference factors and filters them out to facilitate accurate vital signs monitoring during sleep.

In particular, we employ a threshold-based approach to determine whether a segment of CSI measurements contains sleep events/environmental changes or not by examining the short-time energy of the moving variance of the CSI measurements. The rationale behind this is that the sleep events or environmental changes involving large body movements (e.g., going to bed and turn over) result in much larger changes of CSI measurement than that of minute movements of breathing and heart beat. The large movements thus can be detected once the variance energy of the corresponding CSI measurements exceeds a particular threshold.

We denote the CSI samples of  $P$  subcarriers as  $C = [C_1, \dots, C_P, \dots, C_P]'$ , where  $C_p = \{c_p(1), \dots, c_p(T)\}$  represents  $T$

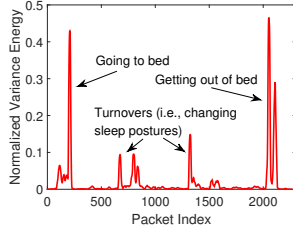


**Figure 9: Short time energy of the variance of difference sleep events.**

CSI amplitudes on the  $p^{\text{th}}$  subcarrier. We further denote the moving variances of the  $P$  subcarriers as  $V = [V_1, \dots, V_p, \dots, V_P]'$ , where  $V_p = \{v_p(1), \dots, v_p(T)\}$  are the moving variances derived from  $C_p$ . Our system can then calculate the cumulative moving variance energy of CSI samples accessing  $P$  subcarriers as:

$$E = \frac{1}{NP} \sum_{p=1}^P \sum_{n=1}^N |v_p(n)|^2, \quad (4)$$

where  $N$  denotes the window length of short time energy.

We empirically determine the variance energy to be 0.02 as the threshold in this work. Figure 9 illustrates the normalized moving variance energy of CSI measurements that are collected when the participant involves different sleep events during sleep. We observe that all sleep events generate significantly large variance energy comparing to that of the minute movements of only breathing and heart beats.

## 6.2 Regular Sleep Event Identification

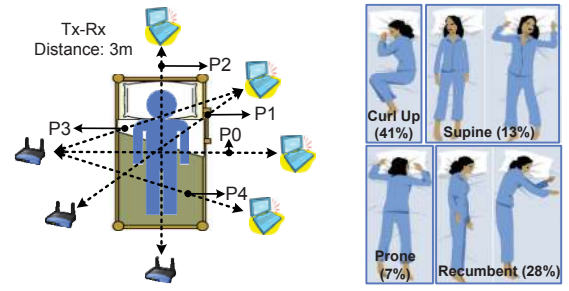
Given the detected sleep events, we further classify them into detailed events such as going to bed, getting off bed and turnovers. Generating statistic of such detailed events can help quantify the sleep quality. For example, frequent getting up or turning overs may suggest that the person has difficulty falling asleep. This information contributes to many healthcare applications such as elderly care and medical diagnosis. As shown in Figure 9, sleep events involving relative larger-scale movements (i.e., going to bed and getting out of bed) result in much larger variance energy than those involving relative smaller-scale movements (i.e., turn overs). We thus can distinguish sleep events with larger-scale movements from those with smaller-scale movements by comparing the variance energy from Equation (4). To further distinguish larger-scale movements, we can exploit the changes of the number of persons in bed to infer these two events. The number of persons in bed can be obtained by using a profile based approach as studied in existing work (e.g., [23]).

## 7. PERFORMANCE EVALUATION

In this section, we evaluate our system of tracking vital signs during sleep in both lab and two apartments.

### 7.1 Device and Network

We conduct experiments in an 802.11n WiFi network with a single off-the-shelf WiFi device (i.e., Lenovo T500 Laptop) connected to a commercial wireless Access Point (AP) (i.e., TP-Link TL-WDR4300). The laptop runs Ubuntu 10.04 LTS with the 2.6.36 kernel and is equipped with an Intel WiFi Link 5300 card for measuring CSI [24]. Unless mentioned otherwise, the packet transmission rate is set to  $20\text{pkts/s}$ . How the packet rate affects the performance will be discussed in Section 7.5.4. For each packet, we extract CSI



(a) Setup of WiFi device-AP pair with different relative positions.

(b) Different sleep postures in bed [25].

**Figure 10: Setup of relative position of WiFi device and AP and sleeping postures.**

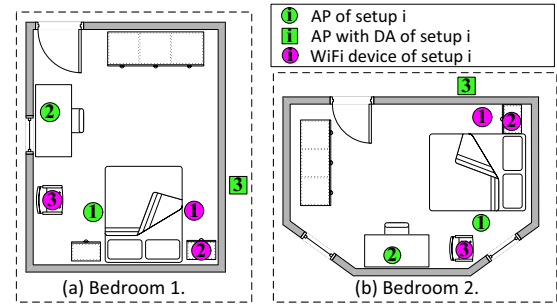


**Figure 11: Two apartment setup.**

for 30 subcarrier groups, which are evenly distributed in the 56 subcarriers of a  $20\text{MHz}$  channel [24].

## 7.2 Experimental Methodology

The experiments are conducted in both lab and two apartments with 6 participants over a three-months time period. The lab environment is a large room with office cubic around. It is used to study the impact of various factors such as obstacles, the various distances between the AP and the WiFi device, and sleep postures. The participants lie on a bed and control their breathing rate to follow various steady beats from a metronome, which is set to a rhythm ranging from  $12\text{bpm}$  to  $18\text{bpm}$ .

We also conduct experiments in two apartments with different bedroom sizes. Figure 11 illustrates the environmental setup in two bedrooms, in which both beds are queen size. The smaller one (i.e., bedroom 1) has the size of about  $12\text{ft} \times 9\text{ft}$ , whereas the larger one (i.e., bedroom 2) is about  $15\text{ft} \times 12\text{ft}$ . As shown in Figure 11, we have three setups in both apartments: setup 1 is the ideal scenario where the AP and WiFi device are placed at two sides of the bed. This setup is useful for persons who want to optimize the performance of the vital signs monitoring during sleep. Setup 2 represents a typical scenario where there is a AP inside the room and a WiFi device, such as smartphone, laptop or tablet, is put on the bed table. Setup 2 has larger distance between the AP and the WiFi device than setup 1. Setup 3 is a challenging scenario where the AP and the WiFi device are placed in different rooms with a concrete wall between them. The distance between the AP and the WiFi device is the largest among three setups. In this setup, we utilize directional antennas (i.e., TL-ANT2406A) to enhance the reception of WiFi signals. The ground truths of breathing and heart rates are monitored by the NEULOG Respiration



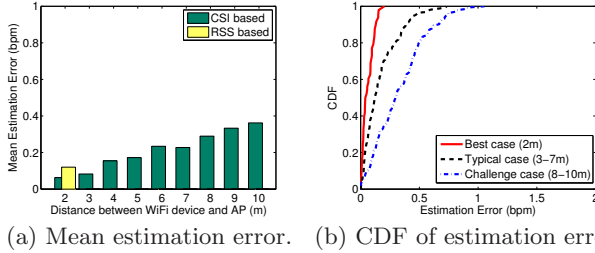


Figure 12: Performance under different distances between WiFi device and AP.

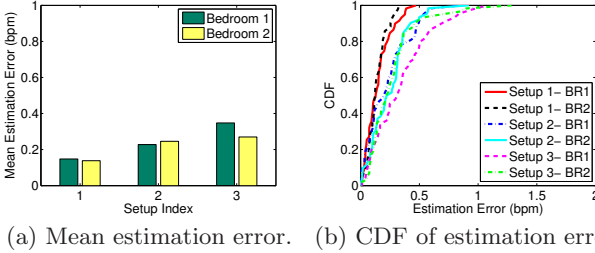


Figure 13: Performance in two real apartments.

Monitor Logger Sensor [22] and a fingertip pulse oximeter, respectively.

### 7.3 Evaluation of Breathing Rate Estimation

We evaluate the overall performance of breathing rate estimation under different scenarios including different distances between the AP and WiFi, evaluation in two real apartments and two persons in bed case.

#### 7.3.1 Effect of Device Distance

As typical bedroom has limited space, we choose a large lab environment to study the performance of breathing rate estimation under various distances. The AP and the WiFi devices are placed at two sides of the bed (i.e.,  $P0$  setup in Figure 10(a)) with distances from 2 to 10 meters. Figure 12(a) presents the mean error in terms of beat per minute (bpm) of breathing rate estimation under different distances when there is a single person in bed. Overall, we observe that the mean estimation error of our breathing rate estimation is lower than  $0.4bpm$ , which demonstrates that our system is very accurate across different distances including very large distances such as 5 to 10 meters. In addition, shorter distance between the AP and the WiFi device results in better performance. For example, the mean error is within  $0.2bpm$  when the distance is under 5 meters. This is because the received WiFi signals are stronger with shorter communication distances, providing more reliable measurements to capture the minute movements of breathing. Comparing to the result of existing work using RSS [10] which only tested with the distance of  $2m$ , as shown in yellow bar in Figure 12(a), our system provides significantly better performance (i.e., the error is reduced by about 67%). Figure 12(b) depicts the Cumulative Density Function (CDF) of the breathing rate estimation error for three categories of distances between the AP and WiFi device: *best case* (i.e.,  $2m$ ), *typical case* (i.e.,  $3m-7m$  covering mid-sized bedrooms), and *challenging case* (i.e.,  $8m-10m$  covering huge-sized bedrooms). As we can see that for both *best case* and *typical case*, over 90% estimation errors are less than  $0.4bpm$ . Even for the *challenging case*, over 80% of estimation errors are smaller than  $0.5bpm$ . This suggests that our system can achieve highly accurate

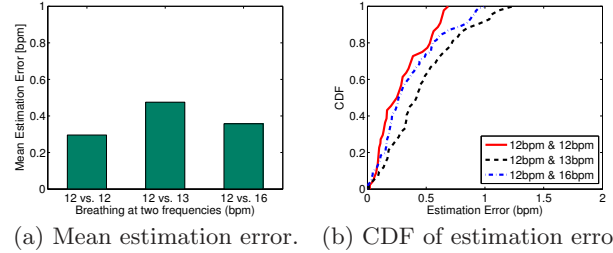


Figure 14: Breathing rate estimation of two persons in bed.

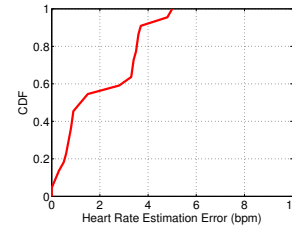


Figure 15: Performance of heart rate estimation.

breathing rate estimation by using a single pair of AP and WiFi device. And it supports large distance between them.

#### 7.3.2 Evaluation in Real Apartments

We next evaluate the breathing rate estimation in two different-size apartment bedrooms with different deployments of the AP and WiFi device, as shown in Figure 11. Figure 13(a) presents the mean estimation error for each setup in two bedrooms. We find that the setup 1 achieves the lowest estimation error of about  $0.15bpm$  in both bedrooms due to the shortest distance between the AP and WiFi device. The estimation error of setup 2 increases as the distance between two devices increases. Still, setup 2 has the estimation error as low as  $0.22bpm$  and  $0.24bpm$  in bedroom 1 and bedroom 2, respectively. In addition, we observe that although setup 3 involves the obstacle (i.e., a 6-inch wall) that blocks the line-of-sight signal transmission and longer distance between the AP and WiFi device, we can still achieve less than  $0.3bpm$  mean estimation error with a single pair of AP and WiFi device. Moreover, Figure 13(b) shows that more than 80% estimation errors are less than  $0.5bpm$  for all of those three setups in two real bedrooms, indicating that our system is accurate and robust in real apartment environments. The above results show that our system provides effective breathing rate monitoring under various distances of WiFi device and AP and is robust across different environments.

#### 7.3.3 Two Persons in Bed Case

We further test our system with two persons in bed using bedroom 1 setup. The AP and WiFi device are placed at two sides of the bed with the distance of  $3m$ . Two participants are breathing with different rates as:  $\{12bpm, 12bpm\}$ ,  $\{12bpm, 13bpm\}$  and  $\{12bpm, 16bpm\}$ . Figure 14 depicts the mean estimation error and the CDF of the breathing estimation error. We observe that the mean error is within  $0.5bpm$  for all combination of different breathing rates. In addition, we find that over 90% of estimation errors are less than  $1bpm$ , which is comparable to that of commercial physical contact devices (e.g., zephyr[26]). Given that we only use a single pair of AP and WiFi device, such accuracy of breathing rate monitoring is very encouraging.



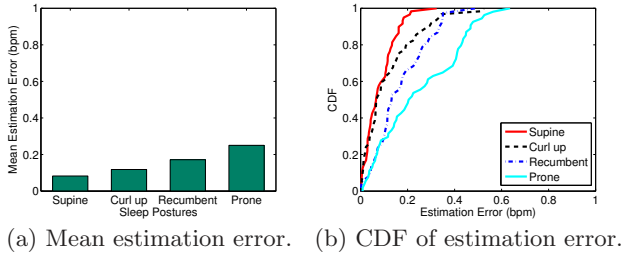


Figure 16: Effect of sleep postures.

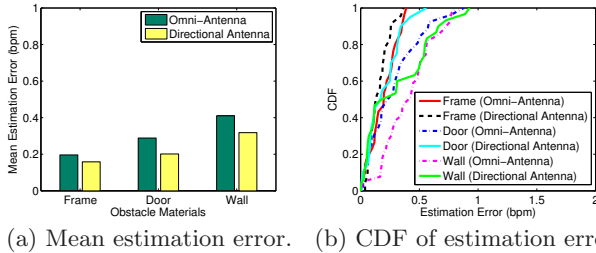


Figure 17: Effect of obstacle between WiFi device and AP.

## 7.4 Performance of Heart Rate Estimation

Figure 15 illustrates the CDF of heart rate estimation error when one person is in bed using setup 1 in bedroom 1 with the AP equipped with directional antennas. We observe that about 57% of estimation errors are less than  $2bpm$  and over 90% of estimation errors are less than  $4bpm$ . The results are very encouraging as our system achieves comparable accuracy to that of commercial sensors, e.g., Zephyr [26] and SleepIQ [15]. Comparing with these commercial products, our system re-uses existing WiFi network without dedicated/wearable sensors or additional cost. Our system thus is able to support large-scale deployment and long-term vital signs monitoring in non-clinical settings. To the best of our knowledge, our work is the first to achieve device-free heart rate estimation leveraging off-the-shelf WiFi.

## 7.5 Impact of Various Factors

In this subsection, we perform detailed study of breathing rate estimation under various factors.

### 7.5.1 Sleep Postures

We experiment with different sleep postures as shown in Figure 10(b). The AP and laptop are placed at two sides of the bed with the distance of  $3m$ . Figure 16(a) compares the mean error of breathing rate estimation resulted from different sleep postures. Overall, our system achieves less than  $0.3bpm$  mean error for all sleep postures, which demonstrates the effectiveness and robustness of our system. In particular, the mean estimation errors of supine, curl up, and recumbent positions are about  $0.07bpm$ ,  $0.1bpm$  and  $0.15bpm$ , respectively. Figure 16(b) shows the CDF curves of estimation error for all postures. We find that our system can obtain less than  $0.2bpm$  error for more than 80% of typical sleep postures. The prone posture has the largest mean estimation error of about  $0.25bpm$  for the reason that the body movements, which are caused by breathing, are mainly in the chest and belly and would be absorbed and blocked by the soft mattress. Still, our system achieves 93% of estimation errors less than  $0.5bpm$  for prone posture.

### 7.5.2 Obstacles/Walls

We evaluate our system with obstacles of different materials in between of AP and WiFi device with  $P0$  deployment in

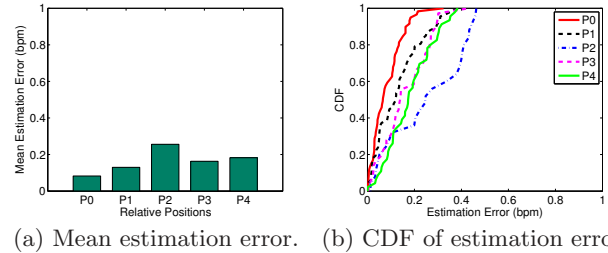


Figure 18: Effect of relative position of WiFi device and AP.

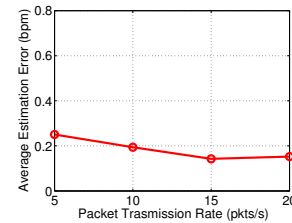


Figure 19: Effect of packet transmission rate.

Figure 10(a). These obstacles are commonly used materials in home environments including a plastic frame of  $1inch$ , a solid wood door of  $2inches$ , and a concrete wall of  $6inches$ . As more and more people use directional antenna to boost the wireless signal reception in home WiFi network, we use both directional and omnidirectional antennas in the experiments. From Figure 17(a), we observe that the mean error is less than  $0.4bpm$  for all materials. Obviously, with the concrete wall, the performance is slightly worse than that of door and plastic frame. In addition, by using the directional antenna, the mean error decreases about  $0.1bpm$ , indicating the directional antenna can enhance the performance of breathing rate estimation due to stronger received signals. Figure 17(b) shows the CDFs of estimation error. We observe that the error is always within  $0.5bpm$  and  $1bpm$  for the plastic frame and wall respectively. The results show that our system can work under different obstacles and the directional antenna could improve the performance. A more comprehensive study of the system performance in various environments with more obstacles and walls will be presented in our future work.

### 7.5.3 Relative Position of WiFi device and AP

Figure 18(a) shows the mean error of breathing rate estimation under different relative positions of Tx-Rx pair (i.e., the AP and WiFi device), as shown in Figure 10(a). We find that the deployment  $P2$  has the largest mean error at about  $0.26bpm$  among all deployments (i.e.,  $P0, P1, P2, P3, P4$ ) since the WiFi signals are partially blocked by the human body (i.e., head and feet). In addition, Figure 18(b) depicts the CDFs of breathing rate estimation errors. We observe that the estimation errors are all within than  $0.5bpm$  even for the worst case deployment  $P2$ . Above results show that our system is effective under different relative positions of WiFi device-AP pair.

### 7.5.4 Packet Transmission Rate

As higher packet transmission rate results in more CSI measurements for vital signs monitoring, we are interested in how the packet rate affects the performance of our system. Furthermore, we study whether our system can work with existing WiFi beaconing packets. Figure 19 presents the mean breathing rate estimation error versus packet transmis-

sion rate when varying the transmission rate from  $5\text{pkt/s}$  to  $20\text{pkt/s}$  using the dataset from apartment experiment (i.e., Bedroom 1, setup 1). We observe that high packet transmission rate slightly improves the performance. Overall, our system is not very sensitive to packet transmission rate, given the range from  $5\text{pkt/s}$  to  $20\text{pkt/s}$ . Specifically, when the packet transmission rate is as low as  $5\text{pkts/s}$  or  $10\text{pkts/s}$ , our system has about  $0.24\text{bpm}$  and  $0.2\text{bpm}$  mean estimation error, respectively. As the commercial access points have the beaconing of  $10\text{pkts/s}$  to broadcast their SSID, our system is able to use such beacons for accurate breathing rate estimation. These results show that our system can not only work with existing AP beaconing packets but also provide accurate breathing rate monitoring with even less packet rate, such as  $5\text{pkts/s}$ .

## 8. CONCLUSION

In this paper, we show that the WiFi network could be exploited to track vital signs during sleep including breathing and heart rates using only one AP and a single WiFi device. In particular, our system exploits fine-grained channel state information from off-the-shelf WiFi devices to detect the minute movements associated with breathing and heart-beat activities. Our algorithms grounded on CSI information in both time and frequency domain have the capability to estimate the breathing rate of a single person as well as two-person in bed cases. Extensive experiments in both lab and two apartments over a three-month time period confirm that our proposed approach using the existing WiFi network can achieve comparable or even better accuracies as compared to existing dedicated sensor based approaches. This WiFi-based approach opens up a new direction in performing device-free and low-cost vital sign monitoring during sleep in non-clinical settings.

## 9. ACKNOWLEDGEMENT

We thank our shepherd, Dr. Lili Qiu, and the anonymous reviewers for their insightful feedbacks. This work was partially supported by the National Science Foundation Grants CNS-1217387, SES-1450091, CNS-1464092 and CNS-1318748.

## 10. REFERENCES

- [1] "Sleep apnea: What is sleep apnea?" *NHLBI: Health Information for the Public. U.S. Department of Health and Human Services*, 2010.
- [2] P. X. Braun, C. F. Gmachl, and R. A. Dweik, "Bridging the collaborative gap: Realizing the clinical potential of breath analysis for disease diagnosis and monitoring—tutorial," *IEEE Sensors Journal*, vol. 12, no. 11, pp. 3258–3270, 2012.
- [3] G. S. Chung, B. H. Choi, K. K. Kim, Y. G. Lim, J. W. Choi, D.-U. Jeong, and K. S. Park, "Rem sleep classification with respiration rates," in *6th International Special Topic Conference on Information Technology Applications in Biomedicine (ITAB)*. IEEE, 2007, pp. 194–197.
- [4] C. A. Kushida, M. R. Littner, T. Morgenthaler, C. A. Alessi, D. Bailey, J. Coleman Jr, L. Friedman, M. Hirshkowitz, S. Kapen, M. Kramer *et al.*, "Practice parameters for the indications for polysomnography and related procedures: an update for 2005," *Sleep*, vol. 28, no. 4, pp. 499–521, 2005.
- [5] Y. Chen, D. Misra, H. Wang, H.-R. Chuang, and E. Postow, "An x-band microwave life-detection system," *IEEE Transactions on Biomedical Engineering*, vol. 33, no. 7, pp. 697–701, 1986.
- [6] J. Salmi and A. F. Molisch, "Propagation parameter estimation, modeling and measurements for ultrawideband mimo radar," *IEEE Transactions on Antennas and Propagation*, vol. 59, no. 11, pp. 4257–4267, 2011.
- [7] F. Adib, Z. Kabelac, H. Mao, D. Katabi, and R. C. Miller, "Demo: Real-time breath monitoring using wireless signals," in *MobiCom*, 2014.
- [8] F. Adib, Z. Kabelac, and D. Katabi, "Multi-person motion tracking via rf body reflections," *MIT technical report*, 2014.
- [9] N. Patwari, L. Brewer, Q. Tate, O. Kaltiokallio, and M. Bocca, "Breathfinding: A wireless network that monitors and locates breathing in a home," *IEEE Journal of Selected Topics in Signal Processing*, vol. 8, no. 1, pp. 30–42, 2014.
- [10] O. J. Kaltiokallio, H. Yigitler, R. Jäntti, and N. Patwari, "Non-invasive respiration rate monitoring using a single cots tx-rx pair," in *IPSN*, 2014, pp. 59–70.
- [11] Fitbit, <http://www.fitbit.com/>.
- [12] Jawbone Up, <https://jawbone.com/up>.
- [13] Sleep as Android, <https://sites.google.com/site/sleepasandroid/>.
- [14] T. Hao, G. Xing, and G. Zhou, "isleep: unobtrusive sleep quality monitoring using smartphones," in *Sensys*, 2013.
- [15] SleepIQ, <http://bamllabs.com/>.
- [16] J. Penne, C. Schaller, J. Hornegger, and T. Kuwert, "Robust real-time 3d respiratory motion detection using time-of-flight cameras," *International Journal of Computer Assisted Radiology and Surgery*, vol. 3, no. 5, pp. 427–431, 2008.
- [17] Y. Wang, J. Liu, Y. Chen, M. Gruteser, J. Yang, and H. Liu, "E-eyes: device-free location-oriented activity identification using fine-grained wifi signatures," in *MobiCom*, 2014, pp. 617–628.
- [18] J. F. Murray, *The normal lung: the basis for diagnosis and treatment of pulmonary disease*. Saunders, 1986.
- [19] P. Sebel, M. Stoddart, R. Waldhorn, C. Waldman, and P. Whitfield, *Respiration, the breath of life*. Torstar Books New York, 1985.
- [20] "Target heart rates - aha," *Target Heart Rates. American Heart Association*, 2014.
- [21] L. Davies and U. Gather, "The identification of multiple outliers," *Journal of the American Statistical Association*, vol. 88, no. 423, pp. 782–792, 1993.
- [22] "NEULOG Respiration Monitor Logger Sensor," <http://www.neulog.com/>.
- [23] W. Xi, J. Zhao, X. Li, K. Zhao, S. Tang, X. Liu, and Z. J., "Electronic frog eye: Counting crowd using wifi," in *INFOCOM*, 2014.
- [24] D. Halperin, W. Hu, A. Sheth, and D. Wetherall, "Tool release: gathering 802.11 n traces with channel state information," *ACM SIGCOMM Computer Communication Review*, vol. 41, no. 1, pp. 53–53, 2011.
- [25] "Sleep position gives personality clue," 2003, <http://news.bbc.co.uk/2/hi/health/3112170.stm>.
- [26] Zephyr Technology, <http://zephyranywhere.com/>.